Chem. Mater. **2007,** *19,* 6150–6157

pH-Sensitive Nanostructural Transformation of a Synthetic Self-Assembling Water-Soluble Tripeptide: Nanotube to Nanovesicle

Partha Pratim Bose,[‡] Apurba Kr. Das,[‡] Raghurama P. Hegde,[§] Narayanaswami Shamala,[§] and Arindam Banerjee*,[†,‡]

Chemistry Division, Indian Institute of Chemical Biology, Jadavpur, Kolkata 700032, India, Indian Association for the Cultivation of Science, Jadavpur, Kolkata 700032, India, and Department of Physics, Indian Institute of Science, Bangalore 560012, India

Received June 18, 2007. Revised Manuscript Received August 2, 2007

Construction of various nanostructures using suitable self-assembling molecular building blocks is a challenging issue. Moreover, controlling the formation of a specific nanostructure from self-assembling molecular building blocks by tuning the pH of the solution is interesting. The present study demonstrates pH-responsive nanostructural transformation of a self-assembling water-soluble tripeptide from nanotubes to nanovesicles. In acidic pH (pH 4.3–5.5), hollow nanotubular structures have been observed, while at pH 6.5 (nearly neutral), both nanotubes and nanovesicles coexist uniformly. With an increase in the pH of the solution, only one nanoscopic species, i.e., nanovesicles, has been formed exclusively, and these hollow, fusible nanovesicles are stable within the range pH 7.0–9.2. A further increase in the pH triggers the rupture of these nanovesicles. pH-sensitive nanovesicle formation has been utilized for the entrapment and slow release of a physiological dye, Congo red.

Introduction

Controlled self-assembly of molecular structures is an interesting topic of recent research in materials science and biology. The key elements in molecular self-assembly are chemical complementarity and structural compatibility. The formation of well-defined nanoscopic architecture with specific shape and size is only achievable by precise control of the molecular arrangement at the supramolecular level.[1] Stupp et al. introduced a supramolecular additive based on the dendron rod coil molecules to modify the supramolecular structure and the function of a polystyrene-based polymer.[2] Zhang and co-workers have developed several surfactant-like peptides that could undergo self-assembly to form nanotubes and nanovesicles having a range of diameters of 30–50 nm. Studies on peptide-based surfactant molecules have significant implications in the design of self-assembling nonlipid biological surfactants.[3] The formation of triple-helical nanofibers of a specific handedness from self-assembling discotic molecules is another interesting example

of controlled self-assembly.[4] There is a unique example of the controlled molecular self-assembly process of an amide-based organic amphiphile that leads to the formation of spherical growth as well as tubular growth by tuning the pH of the solution to obtain a combined structure.[5] Some recent examples of nanostructural transformation include spherical to tubular or cylindrical assemblies by varying the self-assembling structural units.[6] Ghadiri and co-workers have pioneered research on cyclic peptide-based nanotube formation and demonstrated their use as ion and molecular channels.[7] Gazit et al. have demonstrated the structural switching of diphenylalanine-based nanotubes to nanospheres by introducing a thiol group at the end of the diphenylalanine peptide.[8] There are a few examples of peptide-based nanostructural transformations including pH-responsive nanotubes to nanoribbons[9a] and concentration-dependent nanotubes to nanovesicles, using the regulated self-assembly of a single peptide molecule.[9b] However, controlling the self-assembly of a short peptide into nanotubes and the smooth transformation of these nanotubes into nanovesicles by tuning the pH

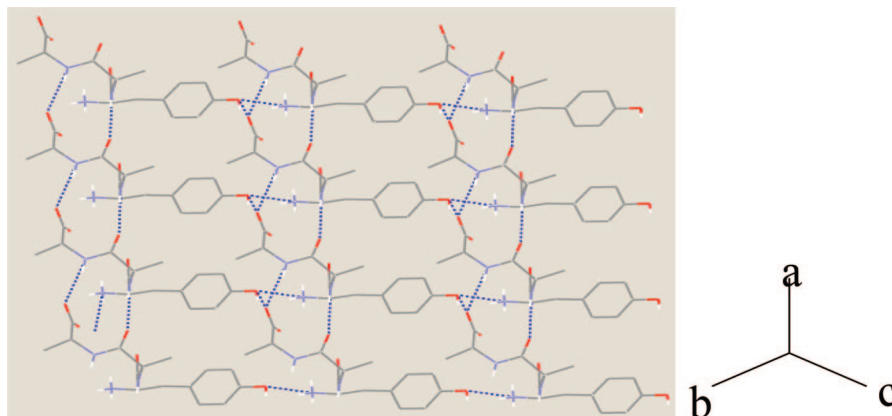* E-mail: arindam.bolpur@yahoo.co.in and arindam@iicb.res.in. Fax: (+) 91-33-2473-5197.
† Indian Institute of Chemical Biology.
‡ Indian Association for the Cultivation of Science.
§ Indian Institute of Science.

(1) (a) Fairman, R.; Àkerfeldt, K. S. *Curr. Opin. Struct. Biol.* **2005,** *15,* 453–463. (b) Vriezema, D. M.; Hoogboom, J.; Velonia, K.; Takazawa, K.; Chirstianen, P. C. M.; Maan, J. C.; Rowan, A. E.; Nolte, R. J. M. *Angew. Chem., Int. Ed.* **2003,** *42,* 772–776. (c) Diaz, N.; Simon, F.-X.; Rawiso, M.; Decher, G.; Jestin, J.; Mésini, P. *Angew. Chem., Int. Ed.* **2005,** *44,* 3260–3264.
(2) (a) Stendahl, J. C.; Zubarev, E. R.; Arnold, M. S.; Hersam, M. C.; Sue, H.-J.; Stupp, S. I. *Adv. Funct. Mater.* **2005,** *15,* 487–493. (b) Zubarev, E. R.; Pralle, M. U.; Sone, E. D.; Stupp, S. I. *Adv. Mater.* **2002,** *14,* 198–203.
(3) (a) Santoso, S.; Hwang, W.; Hartman, H.; Zhang, S. *Nano Lett.* **2002,** *2,* 687–691. (b) von Maltzahn, G.; Vauthy, S.; Santoso, S.; Zhang, S. *Langmuir* **2003,** *19,* 4332–4337.

(4) Bose, P. P.; Das, A. K.; Drew, M. G. B.; Banerjee, A. *Chem. Commun.* **2006,** 3196–3198.
(5) (a) Matsui, H.; Gologan, B. *J. Phys. Chem. B* **2000,** *104* (15), 3383–3386. (b) Matsui, H.; Holtman, C. *Nano Lett.* **2002,** *2,* 887–889.
(6) (a) Kim, B. S.; Hong, D.-J.; Bae, J.; Lee, M. *J. Am. Chem. Soc.* **2005,** *127,* 16333–16337. (b) Ajayaghosh, A.; Varghese, R.; Mahesh, S.; Praveen, V. K. *Angew. Chem., Int. Ed.* **2006,** *45,* 7729–7732.
(7) (a) Bong, D. T.; Clark, T. D.; Granja, J. R.; Ghadiri, M. R. *Angew. Chem., Int. Ed.* **2001,** *40,* 988–1011. (b) Quesada, J. S.; Isler, M. P.; Ghadiri, M. R. *J. Am. Chem. Soc.* **2002,** *124,* 10004–10005. (c) Quesada, J. S.; Ghadiri, M. R.; Bayley, H.; Braha, O. *J. Am. Chem. Soc.* **2000,** *122,* 11757–11766.
(8) (a) Reches, M.; Gazit, E. *Nano Lett.* **2004,** *4,* 581–585. (b) Gilead, S.; Gazit, E. *Supramol. Chem.* **2005,** *17,* 87–92.
(9) (a) Song, Y.; Challa, S. R.; Medforth, C. J.; Qiu, Y.; Watt, R. K.; Pena, D.; Miller, J. E.; van Swol, F.; Shelnutt, J. A. *Chem. Commun.* **2004,** 1044–1045. (b) Yan, X.; He, Q.; Wang, K.; Duan, L.; Cui, Y.; Li, J. *Angew. Chem., Int. Ed.* **2007,** *46* (14), 2431–2434.

10.1021/cm0716147 CCC: $37.00 © 2007 American Chemical Society
Published on Web 11/07/2007

Figure 1. Hydrogen-bonded supramolecular sheet-like structure obtained from single-crystal X-ray crystallography. Dotted lines indicate hydrogen bonds. Only hydrogen-bonded hydrogen atoms are shown for clarity. Color code: red, oxygen; blue, nitrogen; gray, carbon; white, hydrogen.

of the solution is rare. In our previous work, we established that terminally blocked acyclic tripeptides (Boc-Tyr-X-Tyr-OMe, X = Ile/Val) can be regarded as a new motif for the formation of peptide nanotubes,[10] and in this study, we want to address whether a single tyrosine-containing water-soluble tripeptide is able to form a nanotubular structure or not and also to examine the self-assembly of the reported tripeptide Tyr(1)-Aib(2)-Ala(3) in various pH values. Here, we also demonstrate the entrapment and slow release of a physiological dye, Congo red, using pH-responsive peptide-based nanovesicles.

Experimental Methods

We have synthesized a water-soluble synthetic tripeptide **1** containing an unusual amino acid, α-aminoisobutyric acid (Aib), by conventional solution-phase methodology. The final compound was fully characterized by ^{1}H NMR spectroscopy and mass spectrometry.

Synthesis and Characterization of Peptide 1 (H$_2$N-Tyr-Aib-Ala-COOH). Peptide **1** has been synthesized using conventional solution-phase methodology. The N-terminus was protected by the Boc group and the C-terminus was protected as a methyl ester. Couplings were mediated by dicyclohexylcarbodiimide/1-hydroxybenzotriazole (DCC/HOBT). Deprotection of the methyl ester was performed using the saponification method, and the Boc group was deprotected by trifluoroacetic acid (TFA). The final compound was fully characterized by ^{1}H NMR spectroscopy and mass spectrometry.

(a) Synthesis of Boc-Tyr-OH (2). A solution of L-tyrosine (3.62 g, 20 mmol) in a mixture of dioxane (40 mL), water (20 mL), and 1 M NaOH (20 mL) was stirred and cooled in an ice–water bath. Di-*tert*-butyl pyrocarbonate (4.8 g, 22 mmol) was added, and stirring was continued at room temperature for 6 h. Then the solution was concentrated in vacuum to about 20–25 mL, cooled in an ice–water bath, covered with a layer of ethyl acetate (about 20 mL), and acidified with a dilute solution of KHSO$_4$ to pH 2–3 (Congo red). The aqueous phase was extracted with ethyl acetate, and this operation was done repeatedly. The ethyl acetate extracts were pooled, washed with water, dried over anhydrous Na$_2$SO$_4$, and evaporated in vacuum. The pure material was obtained as a waxy solid.

Yield: 4.78 g (17 mmol, 85%). Anal. Calcd for C$_{14}$H$_{19}$NO$_5$ (281): C, 59.79; H, 6.76; N, 4.98. Found: C, 59.77; H, 6.78; N, 5.03.

(b) Boc-Tyr(1)-Aib(2)-OMe (3). A total of 4.5 g (16 mmol) of Boc-Tyr-OH was dissolved in a mixture of 25 mL of dichloromethane (DCM) in an ice–water bath. H-Aib-OMe was isolated from 4.91 g (32 mmol) of the corresponding methyl ester hydrochloride by neutralization, subsequent extraction with ethyl acetate, and concentration (15 mL), and this was added to the reaction mixture, followed immediately by 3.3 g (16 mmol) of DCC. The reaction mixture was allowed to come to room temperature and stirred for 48 h. DCM was evaporated, residue was taken in ethyl acetate (60 mL), and dicyclohexylurea (DCU) was filtered off. The organic layer was washed with 2 M HCl (3 × 50 mL), brine (2 × 50 mL), and then 1 N sodium carbonate (3 × 50 mL) and brine (2 × 50 mL), dried over anhydrous sodium sulfate, and evaporated under vacuum to yield **3** as a white solid.

Yield: 4.56 g (12 mmol, 75%). ^{1}H NMR (300 mHz, chloroform-*d*, 25 °C, TMS): δ 7.17 (d, ^3J(H,H) = 9 Hz, 2H; aromatic CH), 6.75 (d, ^3J(H,H) = 9 Hz, 2H; aromatic CH), 6.36 (s, 1H, NH), 5.13 (d, ^3J = 5.7 Hz, 1H, NH), 4.15–4.30 (m, 1H, CH), 3.72 (s, 3H, OCH$_3$), 2.86–3.04 (m, 2H, CH$_2$), 1.46 (s, 9H, C(CH$_3$)$_3$), 1.44 (s, 6H, 2 × CH$_3$). Anal. Calcd for C$_{19}$H$_{28}$N$_2$O$_6$ (380): C, 60; H, 7.37; N, 7.37. Found: C, 59.55; H, 7.96; N, 7.4.

(c) Boc-Tyr(1)-Aib(2)-OH (4). To 4.4 g (11.58 mmol) of **3** were added 25 mL of MeOH and 15 mL of 2 M NaOH, and the progress of saponification was monitored by thin-layer chromatography (TLC). The reaction mixture was stirred. After 10 h, methanol was removed under vacuum and the residue was taken in 50 mL of water and washed with diethyl ether (2 × 50 mL). Then the pH of the aqueous layer was adjusted to 2 using 1 M HCl, and it was extracted with ethyl acetate (3 × 50 mL). The extracts were pooled, dried over anhydrous sodium sulfate, and evaporated under vacuum to yield 3.8 g of **4**.

Yield: 3.8 g (10.38 mmol, 89.6%). ^{1}H NMR (300 mHz, DMSO-*d$_6$*, 25 °C): δ 12.27 (b, 1H, COOH), 7.09 (d, ^3J(H,H) = 9 Hz, 2H; aromatic CH), 7.92 (s, 1H, NH), 6.94 (d, ^3J(H,H) = 9 Hz, 2H; aromatic CH), 6.57 (s, 1H, NH), 3.92–3.99 (m, 1H, CH), 2.43–2.77 (m, 2H, CH$_2$), 1.26 (s, 9H, C(CH$_3$)$_3$), 1.24 (s, 6H, 2 × CH$_3$). Anal. Calcd for C$_{18}$H$_{26}$N$_2$O$_6$ (366): C, 59.02; H, 7.10; N, 7.65. Found: C, 59.05; H, 7.07; N, 7.69.

(d) Boc-Tyr(1)-Aib(2)-Ala(3)-OMe (5). A total of 3.7 g (10.11 mmol) of **4** in 10 mL of *N,N*-dimethylformamide was cooled in an ice–water bath. H-Ala-OMe was isolated from 2.92 g (21 mmol) of the corresponding methyl ester hydrochloride by neutralization, subsequent extraction with ethyl acetate, and concentration (15 mL), and it was added to the reaction mixture, followed immediately by

(10) Ray, S.; Haldar, D.; Drew, M. G. B.; Banerjee, A. *Org. Lett.* **2004**, *6* (24), 4463–4465.
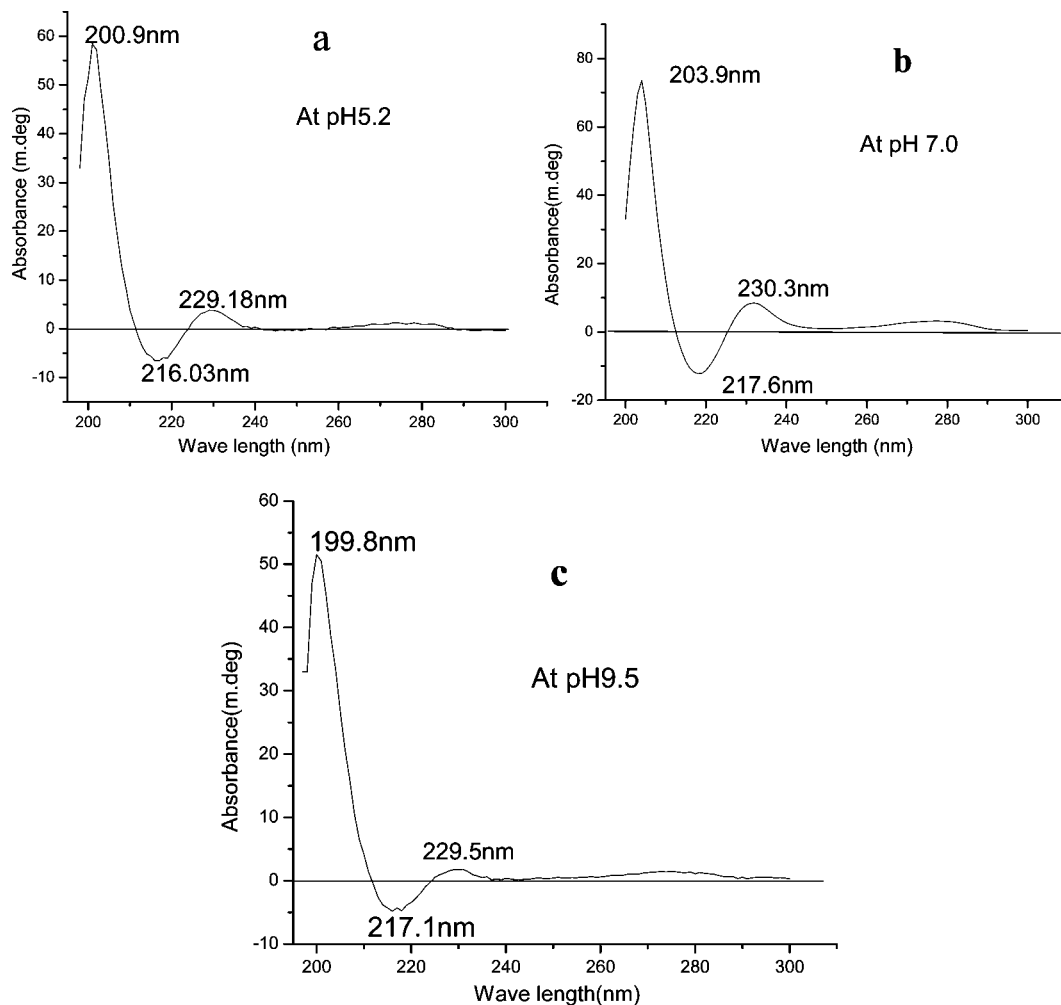
Figure 2. CD spectra of peptide **1** in solutions of pH (a) 5.2, (b) 7, and (c) 9.5.

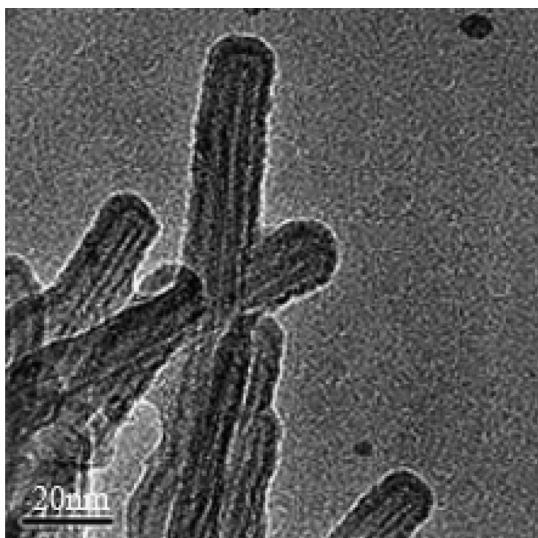**Figure 3.** TEM image of nanotubes at pH 4.3.

Figure 4. TEM image of nanotubes at pH 5.5.

2.08 g (11.11 mmol) of DCC and 1.37 g (10.11 mmol) of HOBT. The reaction mixture was stirred for 3 days. The residue was taken in ethyl acetate (60 mL), and DCU was filtered off. The organic layer was washed with 2 M HCl (3 × 50 mL), brine (3 × 50 mL), 1 M sodium carbonate (3 × 50 mL), and brine (2 × 50 mL), dried over anhydrous sodium sulfate, and evaporated under vacuum to yield peptide **5** as a white solid. Purification was done by a silica gel column (100–200 mesh) using ethyl acetate–toluene (3:1) as the eluent.

Yield: 4.1 g (7.55 mmol, 74.68%). ^{1}H NMR (300 mHz, chloroform-*d*, 25 °C, TMS): δ 7.0 (d, ^3J(H,H) = 9 Hz, 2H; aromatic CH), 6.73 (d, ^3J(H,H) = 9 Hz, 2H; aromatic CH), 6.07 (s, 1H, NH), 5.23 (d, ^3J(H,H) = 6 Hz, 1H; CH), 4.31–4.35 (m, 1H, CH), 3.73 (s, 3H, OCH$_3$), 2.97–3.14 (m, 2H, CH$_2$), 1.43 (s, 9H, C(CH$_3$)$_3$), 1.27 (s, 6H, 2 × CH$_3$). 1.02 (d, 3H, ^3J(H,H) = 6 Hz, CH$_3$). Anal. Calcd for C$_{22}$H$_{33}$N$_3$O$_7$ (451): C, 58.52; H, 7.37; N, 9.31. Found: C, 58.34; H, 7.33; N, 9.28.
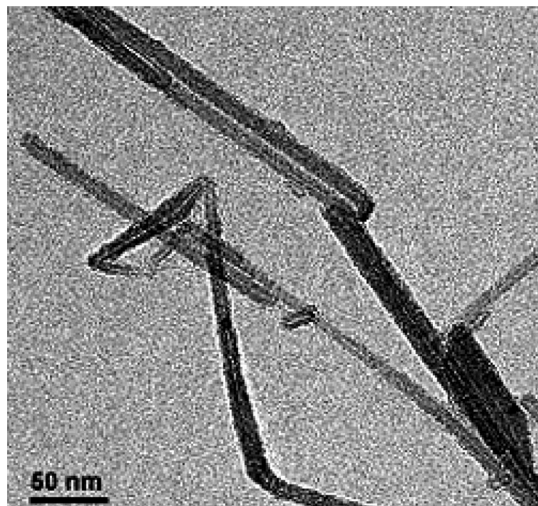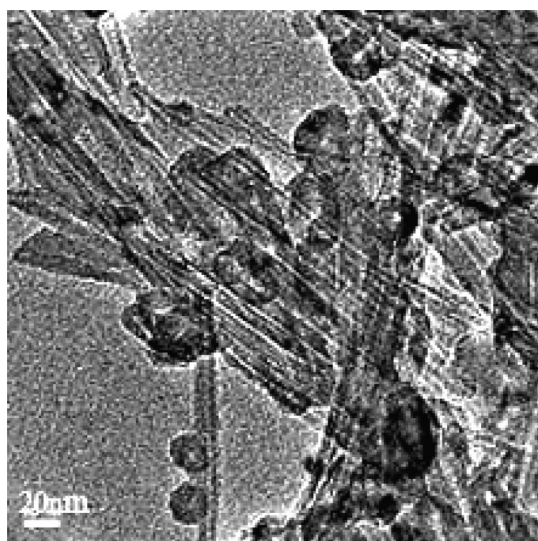
Figure 5. TEM image of nanotubes at pH 6.

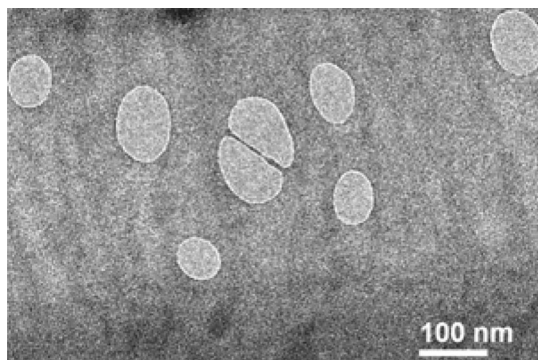**Figure 6.** TEM image showing the coexistence of nanotubes and nanovesicles at pH 6.5.

Figure 7. TEM image of nanovesicles at pH 7.

Figure 8. TEM image of nanovesicles at pH 8.
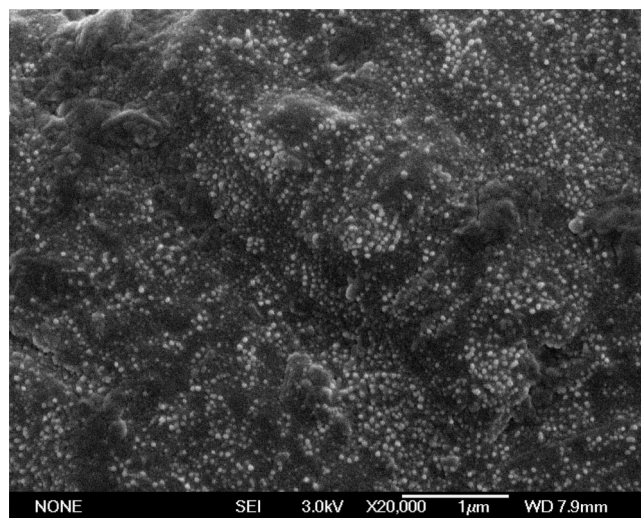
Figure 9. FE-SEM image of nanovesicles at pH 8.
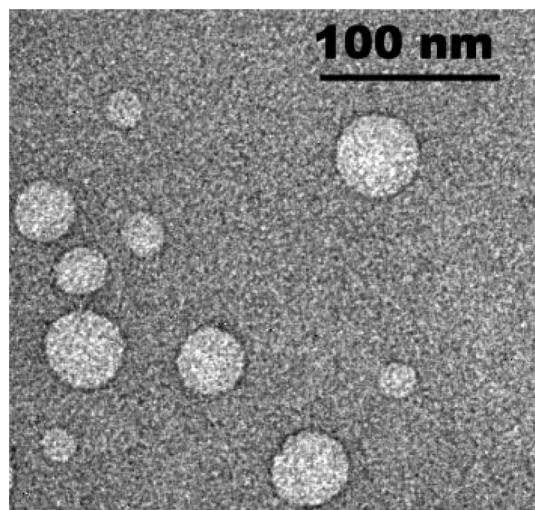
Figure 10. TEM image of nanovesicles at pH 9.2.

(e) Boc-Tyr(1)-Aib(2)-Ala(3)-OH (6). To 3.2 g (4.98 mmol) of peptide **5** were added 25 mL of MeOH and 15 mL of 2 N NaOH, and the progress of saponification was monitored by TLC. The reaction mixture was stirred. After 10 h, methanol was removed under vacuum, and the residue was taken in 50 mL of water and washed with diethyl ether (2 × 50 mL). Then the pH of the aqueous layer was adjusted to 2 using 1 M HCl, and it was extracted with ethyl acetate (3 × 50 mL). The extracts were pooled, dried over
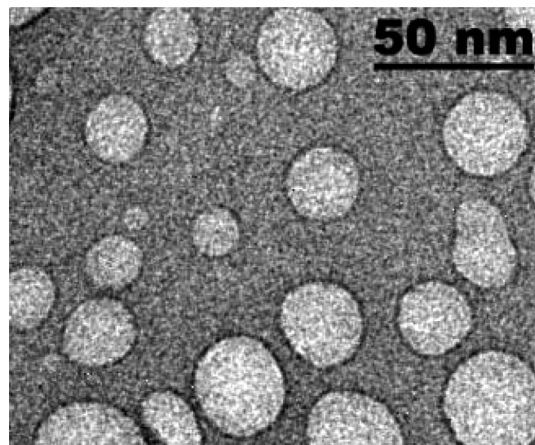
anhydrous sodium sulfate, and evaporated under vacuum to yield as a waxy solid.

Yield: 2.8 g (4.46 mmol, 89.56%). ^{1}H NMR (300 mHz, DMSO-d_6, 25 °C): δ 9.2 (b, 1H, COOH), 8.02 (s, 1H, NH), 7.93 (d, $^3J =$ 8.7 Hz, 1H, NH), 7.04 (d, ^3J(H,H) = 9 Hz, 2H; aromatic CH), 6.89 (d, ^3J(H,H) = 9 Hz, 2H; aromatic CH), 6.75 (d, 1H, $^3J =$ 8.2 Hz, NH), 4.70–4.72 (m, 1H, CH), 4.52–4.54 (m, 1H, CH), 2.78–2.93
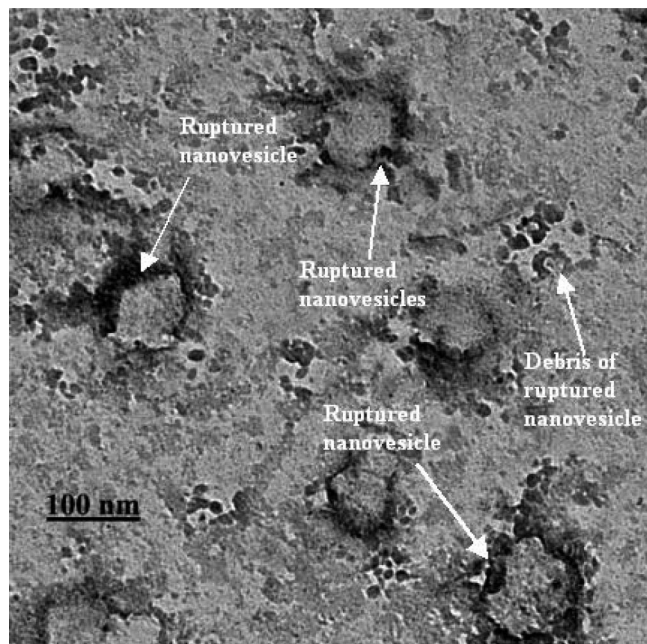
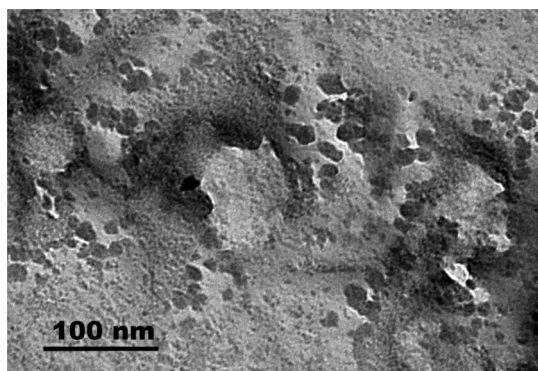**Figure 11.** TEM image of ruptured nanovesicles at pH 10.

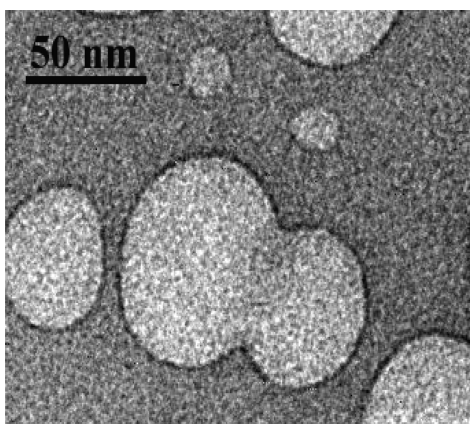**Figure 12.** TEM image of ruptured nanovesicles at pH 11.

Figure 13. TEM image showing vesicle fusion at pH 9.2.

(m, 2H, CH$_2$), 2.06–2.16 (m, 3H, CH$_3$), 1.36 (s, 9H, C(CH$_3$)$_3$), 1.28 (s, 6H, 2 × CH$_3$), 1.03 (d, 3H, ^3J(H,H) = 6 Hz, CH$_3$). Anal. Calcd for C$_{21}$H$_{31}$N$_3$O$_7$ (437): C, 57.65; H, 7.14; N, 9.60. Found: C, 57.66; H, 7.13; N, 9.52.

(f) NH$_3$$^+$-Tyr(1)-Aib(2)-Ala(3)-COO$^-$ (Peptide 1). To 2.7 g (4.3 mmol) of Boc-Tyr-Aib-Ala-OH was added 5 mL of TFA, and the removal of the Boc group was monitored by TLC. After 2 h, TFA was removed under vacuum. The residue was taken in water (20

mL) and washed with diethyl ether (2 × 30 mL). The pH of the aqueous solution was then adjusted to 8 with liquid NH$_3$. The aqueous portion was evaporated under vacuum to yield peptide **1** as a white solid.

Yield: 1.6 g (3.0 mmol, 70.47%). ^{1}H NMR (300 mHz, DMSO-d_6, 25 °C): δ 8.25 (s, 1H, HN), 7.65 (d, ^3J(H,H) = 8.7 Hz, 1H, NH), 7.58 (d, ^3J(H,H) = 8.7 Hz, 1H, NH), 6.67 (d, ^3J(H,H) = 9 Hz, 2H; aromatic CH), 6.60 (d, ^3J(H,H) = 9 Hz, 2H; aromatic CH), 4.42–4.50 (m, 1H, CH), 3.95–3.99 (m, 1H, CH), 2.57–2.72 (m, 2H, CH$_2$), 1.17 (d, 3H, ^3J(H,H) = 6 Hz, CH$_3$). 0.85 (s, 6H, 2 × CH$_3$). Anal. Calcd for C$_{16}$H$_{23}$N$_3$O$_5$ (337): C, 56.96; H, 6.87; N, 12.46. Found: C, 56.89; H, 6.82; N, 12.54. HRMS: *m/z* (%) 360.3315 (20) ([M + Na]$^+$), 361.3310 (20) ([M + Na + H]$^+$).

Circular Dichroic (CD) Study. CD spectroscopy has been carried out on a JASCO J-815-150S instrument at a temperature of 25 °C.

Fourier Transform IR (FT-IR) Spectroscopy. The FT-IR spectra were taken using a Shimadzu (Japan) model FT-IR spectrophotometer. A Nicolet FT-IR instrument [Magna IR-750 spectrometer (series II)] was used to obtain the solid-state FT-IR spectra. For solid-state measurements, the KBr disk technique was used. The experiment was carried out at a temperature of 25 °C.

Transmission Electron Microscopy (TEM) and Field-Emission Scanning Electron Microscopy (FE-SEM). TEM and FE-SEM were carried out to investigate the morphology of the nanostructures. In general, solutions of peptide **1** at different pH values were taken at a concentration of 3 mg/mL, and a drop of that solution was taken in a carbon-coated copper grid (300 mesh) and evaporated to dryness under vacuum for 10 h. With these grids, TEM studies were carried out using a JEOL JEM 2010 electron microscope.

During SEM, a similar solution of peptide **1** was taken on glass coverslips and evaporated to dryness for 24 h. Then, it was studied on a JEOL JSM 6007F instrument at 3.0 kV voltage and 20 000× magnification.

X-ray Crystallography. A colorless needle-shaped crystal, suitable for single-crystal X-ray diffraction study, was obtained from a water–methanol solution by slow evaporation.

Crystal data for peptide **1**, C$_{16}$H$_{23}$N$_3$O$_5$: M = 355.39, hexagonal, spacegroup $P2_1$; single crystals were obtained from a water–methanol solution by slow evaporation. a = 6.196(4) Å, b = 15.428(11) Å, c = 9.697(7) Å, V = 924.1 (11) Å^3, Z = 2, μ = 0.098 mm^{-1}, ρ_{calcd} = 1.277 g cm^{-3}, f(000) = 1812, R1 = 0.0829, wR2 = 0.1951 for 2516 reflections with ($|F_o|$ > 4σ($|F_o|$)). X-ray crystal data were collected on a Bruker AXS SMART Apex CCD diffractometer with Mo Kα (λ = 0.710 73 Å) radiation at 20 °C. The structure was obtained by direct methods using SHELXS-97.[11] The hydrogen atoms were fixed geometrically in ideal positions and refined as riding over the non-hydrogen atoms to which they are bonded.

Results and Discussion

Single-Crystal X-ray Diffraction and Solid-State FT-IR Studies. The tripeptide **1** self-assembles to form a supramolecular sheet structure in crystals (Figure 1). Single-crystal X-ray diffraction analysis of peptide **1** (CCDC 644950) revealed the formation of a sheet-like structure, which is made up of zwitterions of the tripeptide in crystals. Adjacent peptide molecules are joined via the hydrogen bonds between the –NH$_3$$^+$ end of one molecule and the –OH group of the tyrosine moiety of the other molecule to form

(11) (a) Sheldrick, G. M. *Acta. Crystallogr., Sect. A: Fundam. Crystallogr.* **1990**, *46*, 467–473.

Synthetic Self-Assembling Water-Soluble Tripeptide

Chem. Mater., Vol. 19, No. 25, 2007 6155
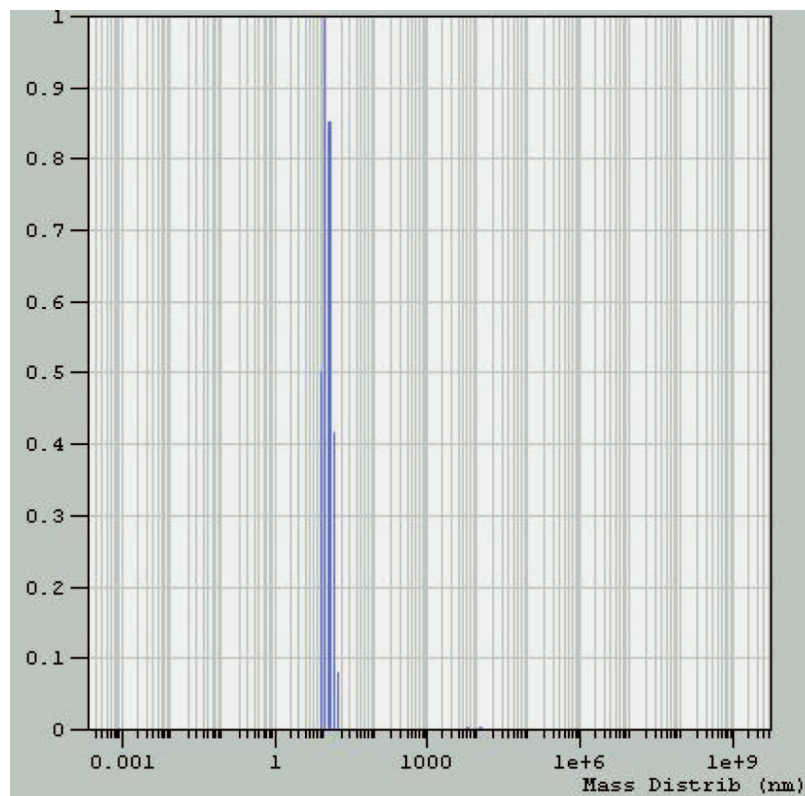
Figure 14. DLS results of peptide **1** at pH 9.2 showing only the distribution of diameters of the nanostructures. The mean diameter of the nanostructures was calculated with the software program *Dynals* and was found to be 10.99 nm.
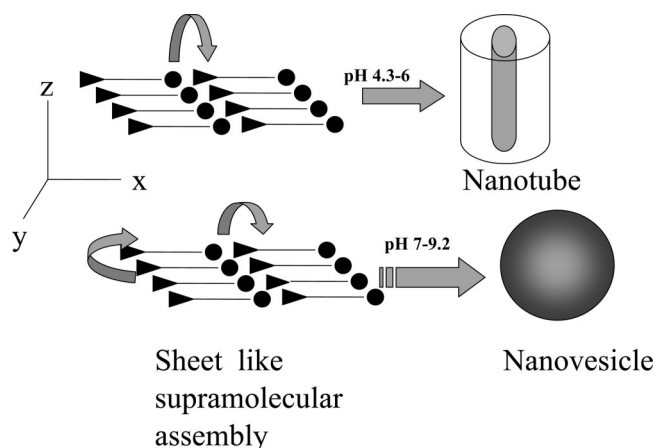
Figure 15. Schematic representation of the possible modes of assembly for the formation of nanotubes and nanovesicles at different pH values.

a molecular strand along the *a* axis, and two adjacent molecular strands are interconnected by the salt bridge interaction of $-NH_3^+$ and $-COO^-$ (Figure 1) to form a hydrogen-bonded sheet-like layered structure utilizing two types of hydrogen bonds, namely, head-to-tail $NH_3^+ \cdots {}^-OOC$ and tyrosine$-OH \cdots {}^-OOC$ along the *ab* plane. These molecular slabs are stacked together by another type of hydrogen bond involving backbone peptide $N-H \cdots OC$ $(N2-H2 \cdots O2)$ along the *a* axis (Figure 1). The zwitterionic nature of peptide **1** has also been supported by the solid-phase FT-IR data of peptide **1**. FT-IR spectra of peptide **1** in its solid state (in KBr) shows the following peaks: COO^-, CO antisym, 1556 cm^{-1}, $-NH_3^+$, 3014.5 cm^{-1} (br) and 1596.9 cm^{-1}; peptide CO stretching, 1620 cm^{-1}; peptide NH stretching and bending, 3277 and 1516 cm^{-1}, respectively.

Interestingly, the last three peaks, i.e., peptide carbonyl stretching and peptide NH stretching and bending, correspond to the formation of a β-sheet structure.[12]

CD Study. Structures of peptide **1** in solutions at different pH values were determined using CD spectroscopy (JASCO J-815-150S) of a solution of peptide **1** at pH 5.2 (Figure 2a), 7 (Figure 2b), and 9.5 (Figure 2c). The solution concentrations were taken as 1.12×10^{-4}, 1.23×10^{-4}, and 1.28×10^{-4} M, respectively. First of all, each of the solutions was heated up to 60 °C and then allowed to cool to 25 °C before the CD experiments were carried out. All of these CD spectra have a common feature, indicating the presence of a β-sheet structure irrespective of the pH of the solution. CD spectra of peptide **1** in all pH values under investigation had a positive band in the range of 229–230 nm, which was certainly due to the participation of an aromatic side chain of the tyrosine residue, while the negative peaks at 216.03, 217.6, and 217.1 nm with positive peaks at 200.9, 203.9, and 199.8 nm, respectively, suggest the formation of a β-sheet structure at the corresponding pH.[13]

TEM and FE-SEM. To investigate the nanostructural features of tripeptide **1**, we examined the TEM images of peptide **1** in solutions of various pH values. Peptide **1** (5 mg) and 1 mL of buffer at pH 4.3, containing only 5% methanol (v/v) as the cosolvent, were mixed in a sealed test tube, and the mixture was continuously stirred for 0.5 h at 60 °C. The mixture was then cooled at room temperature

(12) Banerjee, A.; Das, A. K.; Drew, M. G. B.; Banerjee, A. *Tetrahedron* **2005**, *61*, 5906–5914.
(13) Woody, R. W. *Eur. Biophys. J.* **1994**, *23*, 253–262.
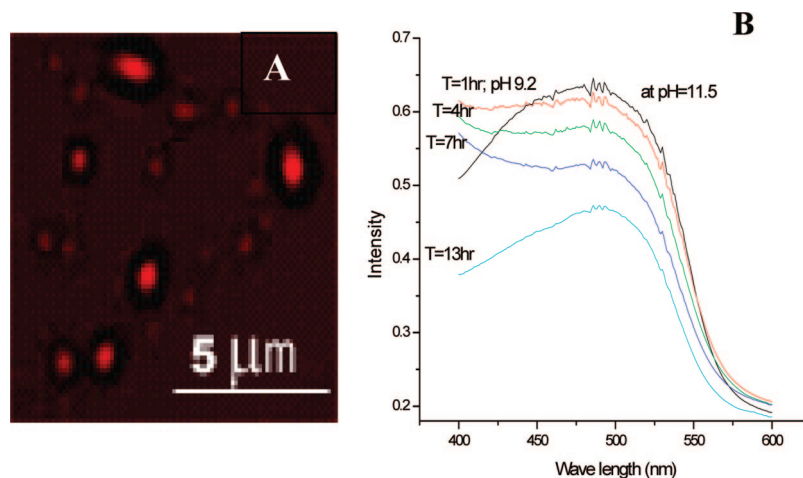
Figure 16. (A) Fluorescence microscopic image showing the entrapment of a physiological dye, Congo red, by nanovesicles at pH 9.2. (B) UV-absorption spectra showing the encapsulation and release of Congo red dye by nanovesicles at different pH values. Red-, green-, indigo-, and sky-blue-colored curves show the gradual absorption of Congo red with respect to time at pH 9.2. The black-colored curve shows the release of the dye at pH 11.5.

and subjected to TEM studies. The TEM images revealed the formation of only peptide nanotubes with an average diameter of 20 nm containing an internal diameter of about 5 nm (Figure 3). At pH 5.5, only nanotubes with an avarage total diameter of 30 nm with an internal diameter of 2 nm have been observed (Figure 4). Exclusive formation of the nanotube has also been observed in the TEM image from the solution of peptide **1** at pH 6 (Figure 5). The nanotube obtained at this pH (pH 6) has a total diameter of 32 nm with an internal diameter of 3 nm. After that, we make the pH of the solution 6.5 by preparing the solution in an acetate buffer solution [with 5% methanol (v/v) as the cosolvent]. Then 5 mg of peptide **1** was dissolved in that acetate buffer–methanol solution, and the resulting solution was subjected to heat treatment as before. The formation of nanotubes with an average total diameter of 25 nm containing an internal diameter of 5 nm and some coexistent nanovesicles with diameters ranging from 20 to 32 nm was observed this time (Figure 6). After that, TEM experiments were carried out at the neutral pH [pH 7, containing 5% methanol (v/v)] using these peptide **1** solutions, and it was found that only nanovesicles were formed with the diameters ranging from 50 to 85 nm (Figure 7). To investigate the nanoscopic feature of peptide **1** at basic pH, we repeated the experiment at pH 8 and 9.2 with Tris buffer (with 5% methanol as the cosolvent). This time, the TEM images revealed that only nanovesicles were formed at those pH values (pH 8 and 9.2) in the diameter ranges of 10–40 and 10–60 nm, respectively (Figures 8–10). However, the peptide nanovesicles started rupturing at pH 10 (Figure 11), and it was completed at pH 11 (Figure 12). So, it is evident from the above results that at acidic pH range 4.3–6.0 self-assembly of the peptide **1** molecule leads to the exclusive formation of various hollow nanotubes (Figures 3–5), while nanovesicles are the sole nanostructural feature at the neutral pH (pH 7) and also at the basic pH (pH 7–9.2). At slightly acidic pH (pH 6.5), both nanotubes and nanovesicles are present uniformly, and this suggests that the pH-dependent nanostructural transition occurs across this pH (pH 6.5).

FE-SEM studies have been carried out to examine the three-dimensional morphology of nanovesicles, and the

FE-SEM study demonstrated the exclusive formation of nanovesicles with different diameters (10–25 nm) at pH 9.2 (Figure 9).

Dynamic Light Scattering (DLS). To get the idea about the size distribution of nanovesicles, a DLS experiment was carried out with a solution of peptide **1** in a Tris buffer at pH 9.2 [5% methanol (v/v) as the cosolvent]. Both bigger and smaller nanovesicles have been observed in TEM images (Figure 10). However, DLS data demonstrated the formation of smaller nanovesicles with a distribution of diameters centered on 11 nm (Figure 14). Larger nanovesicles are formed from the fusion of the smaller nanovesicles, and this is illustrated in Figure 13.

Formation of Nanotubes and Nanovesicles from the β-Sheet Structure. It was evident from the TEM images of the peptide samples at pH 4.3, 5.5, and 6 that the self-assembling peptide **1** molecule indeed forms various nanotubular structures at those pH values. At the pH range 4.3–9.2, because of ionization of the carboxylic acid group and the formation of $-NH_3^+$ species, the molecule of peptide **1** exists as a zwitterion, which can be self-assembled to form a sheetlike structure. It is evident from the crystal structure and CD data that in both acidic and basic pH (pH 4.2–9.2) the peptide **1** molecule self-assembles to form supramolecular β-sheets. In acidic pH (pH 4.2–6.5), nanotubes have been observed in TEM images. Folding of the layered β-sheet structure leads to the formation of a nanotube, and an analogy can be drawn with the formation of carbon nanotubes from a carbon-layered structure.[14] However, at neutral and basic pH (pH 7–9.2), only nanovesicles were observed in TEM. It is only possible if we consider the closure of the supramolecular β-sheet structure in two different directions simultaneously, and this is illustrated in Figure 15. However, the exact reason for the formation of only nanovesicles in basic pH is yet to be explored. At pH 10, rupturing of these vesicles has been observed from TEM

(14) Tenne, R. *Angew. Chem., Int. Ed.* **2003**, *42*, 5124–5132.
(15) (a) Klyachko, V. A.; Jackson, B. *Nature* **2002**, *418*, 89–92. (b) Braell, W. A. *Proc. Natl. Acad. Sci. U.S.A.* **1987**, *84*, 1137–1141.

Synthetic Self-Assembling Water-Soluble Tripeptide

Chem. Mater., Vol. 19, No. 25, 2007 **6157**

images (Figure 11). This is probably due to the ionization of the phenolic –OH side chain of the tyrosine residue as well as the deprotonation of the backbone $–NH_3^+$ group present in peptide **1**, which, in turn, destabilized the sheet structure as a result of charge–charge repulsion.

Encapsulation of Dye (Congo Red) and Its Release. The nanovesicles were efficient in encapsulating physiological dye Congo red, and Figure 16A clearly demonstrates the entrapment of Congo red at pH 9.2 using these nanovesicles. An aqueous solution (2 mg/mL) of the Congo red dye was added into the nanovesicles, and the dye molecules were gradually absorbed by these nanovesicles during a period of 13 h. This phenomenon was evident from the gradual decrease in the intensity of the UV absorption spectra of Congo red (Figure 16A). The phenomenon of the rupturing of nanovesicles by enhancement of the pH (from pH 9.2 to 11.0) can be utilized for the release of the dye Congo red. When the pH of the same solution was adjusted to 12, after 13 h, all entrapped dye molecules got released and the intensity of UV spectrum regained its initial value. The release of an entrapped dye molecule at pH 12 can be justified by the breakage of these nanovesicles at pH 12 (Figure 16B).[15]

Conclusion

In conclusion, it can be stated that it is a unique example of pH-sensitive control of the self-assembly of a short peptide that leads to the formation of a specific nanostructure, such as hollow nanotubes at the acidic pH (pH 4.3–6.0), the formation of both nanotubes and nanovesicles at pH 6.5, and also the formation of only nanovesicles at pH 7–9.2. Thus, pH regulation can be used as an external stimuli not only to control the self-assembly for the formation of a specific nanostructure but also to direct the transition of one nanostructure to the other. The study of vesicle fusion is an area of intense current research interest.[15] The nanovesicle formed in the basic pH showed interesting fusion phenomena, and these peptide-based vesicles thus may be utilized for the model study of the formation, transport, and targeted fusion of endosomal vesicles in cell-free conditions. The property of pH responsiveness for the formation and fusibility of the nanovesicles can be endowed with a probable use of the nanovesicles as vehicles for the delivery of biologically important molecules.[15,16]

(16) Ghosh, S.; Meital, R.; Gazit, E.; Verma, S. *Angew. Chem., Int. Ed.* **2007**, *46*, 2002–2004.